



OPEN ACCESS

EDITED BY
Christoph Hölscher,
Research Center Borstel (LG), Germany

REVIEWED BY
Ana Raquel Maceiras,
Gulbenkian Institute for Molecular
Medicine, Portugal
Kristina Ritter,
Research Center Borstel (LG), Germany

*CORRESPONDENCE
Xinchun Chen
✉ chenxinchun@szu.edu.cn
Junyun Huang
✉ 13879789666@163.com

RECEIVED 17 November 2025
REVISED 27 February 2026
ACCEPTED 27 February 2026
PUBLISHED 17 March 2026

CITATION
Li F, Dai Y, Xie S, Hu R, Gao X, Huang X,
Zhong S, Cai Y, Chen X and Huang J
(2026) Distribution of granzyme-
expressing NK cells in tuberculosis
reflects subset and compartment-
specific remodeling.
Front. Immunol. 17:1747972.
doi: 10.3389/fimmu.2026.1747972

COPYRIGHT
© 2026 Li, Dai, Xie, Hu, Gao, Huang,
Zhong, Cai, Chen and Huang. This is an
open-access article distributed under the
terms of the [Creative Commons
Attribution License \(CC BY\)](https://creativecommons.org/licenses/by/4.0/). The use,
distribution or reproduction in other
forums is permitted, provided the
original author(s) and the copyright
owner(s) are credited and that the
original publication in this journal is
cited, in accordance with accepted
academic practice. No use, distribution
or reproduction is permitted which does
not comply with these terms.

Distribution of granzyme- expressing NK cells in tuberculosis reflects subset and compartment- specific remodeling

Fuxiang Li^{1,2}, Youchao Dai³, Shuixiang Xie⁴, Rong Hu^{1,2},
Xueyun Gao⁵, Xiao Huang², Shuxi Zhong², Yi Cai⁶,
Xinchun Chen^{6*} and Junyun Huang^{1,2*}

¹Department of Laboratory Medicine, First Affiliated Hospital of Gannan Medical University, Ganzhou, China, ²The First Clinical Medical College of Gannan Medical University, Ganzhou, China, ³Guangzhou Eighth People's Hospital, Guangzhou Medical University, Guangzhou, Guangdong, China, ⁴School of Basic Medicine, Gannan Medical University, Ganzhou, China, ⁵Department of Chemistry, Faculty of Environment and Life Science, Center of Excellence for Environmental Safety and Biological Effects, Beijing University of Technology, Beijing, China, ⁶Guangdong Provincial Key Laboratory of Infection Immunity and Inflammation, Department of Pathogen Biology, Shenzhen University Medical School, Shenzhen, China

Introduction: Natural killer (NK) cells contribute to immunity against *Mycobacterium tuberculosis* (*Mtb*), yet their granzyme expression and subset distribution in TB remain poorly defined.

Methods: NK cell subsets and the expression of granzymes (GZMA, GZMB, and GZMK) and CCR5 were analyzed by multiparametric flow cytometry in peripheral blood from healthy controls, individuals with latent TB infection, active TB patients, and treated TB patients, as well as in paired pleural fluid samples.

Results: In peripheral blood from active TB patients, NK cells exhibited reduced co-expression of GZMA, GZMB, and GZMK alongside decreased subset frequencies and absolute counts, a defect restored after treatment. In contrast, pleural fluid NK cells exhibited a distinct signature characterized by elevated GZMK but reduced GZMA and GZMB. This pattern was attributable to the relative enrichment of CD56^{bright} NK cells, which are inherently high in GZMK. We also identified a CCR5^{bright} NK cell subset, phenotypically resembling CD56^{bright} NK cells with high GZMK and low GZMA/GZMB expression, that was selectively expanded in peripheral blood of TB patients and enriched in pleural effusions. This subset was inducible by in vitro *Mtb* stimulation of healthy PBMCs.

Discussion: These findings reveal granzyme remodeling and altered distribution of GZMK⁺CD56^{bright} NK cells associated with CCR5^{bright} expression in TB, suggesting their potential involvement in tissue-specific NK responses.

KEYWORDS

CCR5, GZMA, GZMB, GZMK, natural killer cells, tuberculosis

Introduction

Tuberculosis (TB), caused by *Mycobacterium tuberculosis* (*Mtb*), remains one of the leading global health threats, with approximately a quarter of the world's population infected with the pathogen in a latent state (LTBI) (1). While most individuals with LTBI do not progress to active disease, 5–10% may develop TB, particularly those with weakened immune systems (2). Before adaptive immunity against *Mtb* develops, innate immune mechanisms provide the first line of defense. Natural killer (NK) cells are central to this response, they directly eliminate extracellular *Mtb* by releasing perforin, GZMB, and granzysin (3, 4). NK cells also produce cytokines and chemokines, including IFN- γ , TNF- α , IL-5\10\13, and GM-CSF, which influencing TB progression (5). Furthermore, NK cells recognize and induce apoptosis in *Mtb*-infected cells, promote immature dendritic cell maturation (6) and regulate adaptive immunity against *Mtb* by modulating CD8⁺ T cell (7, 8) and regulatory T cell expansion (9, 10). In T cell deficient mice, NK cell depletion leads to higher lung bacterial loads, more severe tissue damage, and reduced survival, highlighting their essential role in early TB defense (11).

Despite these protective functions, clinical evidence indicates that *Mtb* infection alters NK cell frequency, subset distribution, and effector molecules expression (12). Specifically, reductions in total NK cell counts and shifts in NK cell subsets have been observed (13–15), including decreases in CD56^{bright} CD16^{+/-} (16) and CD8 α ⁺ NK cells (17), along with diminished cytotoxicity (18–21). While these alterations are well-documented in peripheral blood, much less is known about NK cell remodeling at infection sites, such as pleural fluid. Granzymes, including GZMA, GZMB, and GZMK, are critical mediators of NK cell cytotoxicity, inducing apoptosis in infected, foreign or tumor cells (22). Recent evidence suggests that granzymes also play a direct or indirect role in suppressing *Mtb* growth (3, 23, 24), highlighting their potential role in antimicrobial defense. However, despite clear evidence of NK cell remodeling during TB, the impact of *Mtb* infection on the dynamic changes in granzyme expression during TB progression and across different anatomical compartments in TB patients remains poorly understood.

Building on previous work from our team, where we found a reduction in the percentage of peripheral blood CD3⁻CD7⁺GZMB⁺ NK subsets in advanced TB (25), and observed differential granzyme expression in CD4⁺ and CD8⁺ NK cells between peripheral blood and pleural effusions in TB patients (24), we sought to investigate the compartment- and disease state-specific remodeling of NK cell granzyme expression in TB. Specifically, we compare the granzyme expression profiles of NK cells in peripheral blood and pleural effusions from HC, LTBI, TB and RxTB. We show that, in peripheral blood, NK cells from TB patients exhibit reduced expression of GZMA, GZMB, and GZMK compared to healthy controls and latent TB, with recovery of these expressions following successful treatment. Conversely, NK cells in pleural fluid demonstrate elevated GZMK but reduced GZMA and GZMB expression, a finding linked to the presence of a CCR5^{bright} NK cell subset. Our study provides new insights into the subset- and compartment-specific remodeling of granzyme-expressing NK cells during TB.

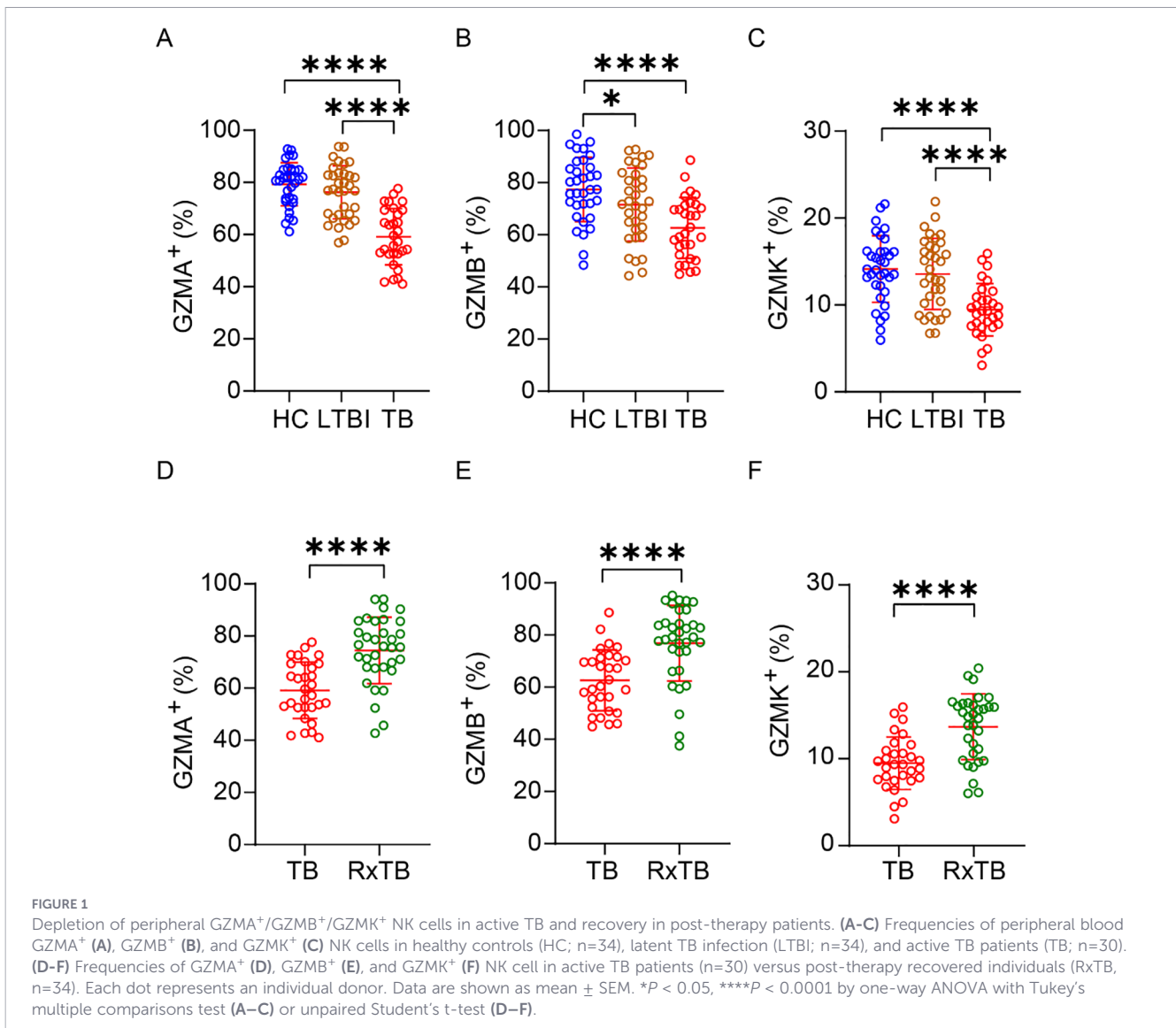
Results

Depletion of peripheral GZMA⁺, GZMB⁺ and GZMK⁺ NK cells in active TB and recovery in post-therapy patients

Multiple studies indicate that NK cell subset composition and key effector molecules are altered during TB progression, and our preliminary work demonstrated reduced CD3⁻CD7⁺GZMB⁺ subsets in advanced TB (25). Given that granzymes are central mediators of NK-cell cytotoxicity against *Mtb*, we investigated whether granzyme expression in NK cells is affected by TB infection. PBMCs from HC, LTBI, active TB patients, and RxTB were analyzed by flow cytometry (Supplementary Figure 1A). To better understand the changes in granzyme-positive NK cells during TB progression, we also quantified the absolute number of circulating NK cells. Consistent with previous reports (13–15), the total number of peripheral blood NK cells was significantly reduced in TB patients compared with HCs (Supplementary Figure 1B). Further analysis revealed that, compared to HCs and LTBI subjects, active TB patients exhibited significantly reduced percentages and absolute numbers of GZMA⁺, GZMB⁺, and GZMK⁺ NK cells (Figures 1A–C, Supplementary Figures 1C–E). After successful anti-TB therapy, both the total NK cell numbers and the frequencies/absolute counts of these granzyme-positive NK subsets showed significant recovery in RxTB patients. (Figures 1D–F, Supplementary Figures 1F–I). These findings demonstrate that expression of GZMA, GZMB and GZMK in peripheral NK cells is closely associated with TB disease progression.

Broad reduction of peripheral NK cell granzyme co-expressing subsets during active TB reverses after treatment

To further characterize the functional landscape of NK cells, we delineated their combinatorial granzyme expression profiles using Boolean gating analysis incorporating GZMA, GZMB, and GZMK. This analysis confirmed that the GZMA⁺GZMB⁺GZMK⁻ phenotype was predominant, whereas GZMA⁺GZMB⁺GZMK⁺ and GZMA⁻GZMB⁺GZMK⁺ populations were infrequent (Figure 2A). Notably, the frequencies of GZMA⁺GZMB⁺GZMK⁺, GZMA⁺GZMB⁺GZMK⁻, and GZMA⁺GZMB⁻GZMK⁺ subsets declined along with TB progression and recovered after successful treatment. In contrast, the percentage of GZMA⁻GZMB⁻GZMK⁻ NK cells increased during active disease and decreased post-therapy (Figures 2A, B). NK cells expressing only a single granzyme (GZMA, GZMB, or GZMK alone) did not show significant changes across disease states (Figures 2A, B). We further quantified the absolute numbers of these granzyme-defined subsets. Consistent with the frequency data, the absolute counts of GZMA⁺GZMB⁺GZMK⁺, GZMA⁺GZMB⁺GZMK⁻, and GZMA⁺GZMB⁻GZMK⁺ NK cells decreased during active TB and restored after treatment (Figures 2C, D), whereas GZMA⁻GZMB⁻GZMK⁻ NK cells showed the opposite trend. Given that human NK cells express multiple other granzymes, it remains unclear whether the expanded GZMA⁻GZMB⁻GZMK⁻ subset in TB expresses other granzyme family members, which warrants further investigation.



These results indicate that GZMA⁺GZMB⁺GZMK⁻ represents the major NK cell subset, highlighting a prevalent co-expression pattern of GZMA and GZMB. In contrast, most GZMK⁺ NK cells co-expressed GZMA but not GZMB (Figures 2A, C), forming distinct GZMK⁺GZMA⁺ and GZMK⁺GZMB⁻ clusters (Supplementary Figure 2). Collectively, these data demonstrate that the progression of active TB is associated with a broad and coordinated reduction in the frequencies and absolute numbers of nearly all granzyme-co-expressing NK cell subsets, which is reversed after treatment. This pattern indicates a generalized impairment of NK cell effector function during active disease, extending beyond the loss of single granzyme-expressing cells.

Peripheral blood and pleural fluid NK cells from TB patients exhibit differing granzyme expression profiles

Tuberculous pleural effusions (TPE), resulting from delayed hypersensitivity to subpleural TB lesions, are enriched in immune cells heavily exposed to *Mtb* antigens (26). To examine how disease-

site NK cells differ from peripheral NK cells, we analyzed paired PBMCs and PFMCs from TB patients (gating strategy shown in Supplementary Figures 3A, B). Flow cytometry analysis revealed a significantly lower frequencies of NK cells in PFMCs compared to PBMCs (Figure 3A). Furthermore, the NK cells in PFMCs exhibited reduced proportions of GZMA⁺ and GZMB⁺ subsets. Quantitatively, the mean frequency of GZMA⁺ NK cells decreased from 58.0% in PBMCs to 42.5% in PFMCs, corresponding to an average reduction of 15.5 ± 4.2% (Figure 3B). A slightly greater reduction was observed for GZMB⁺ NK cells, whose mean frequency declined from 62.8% to 43.9%, representing a decrease of 18.9 ± 4.1% (Figure 3C). In contrast, the GZMK⁺ subsets was markedly enriched in PFMCs, with the mean frequency increasing from 11.5% in PBMCs to 45.9% in PFMCs, corresponding to an average increase of 34.4 ± 3.8% (Figure 3D). Granzyme co-expression profiling further demonstrated that the proportions of GZMA⁺GZMB⁺GZMK⁺, GZMA⁺GZMB⁻GZMK⁺, and GZMA⁻GZMB⁻GZMK⁺ NK subsets were markedly elevated in PFMCs, whereas the GZMA⁺GZMB⁺GZMK⁻ subset was significantly reduced (Figure 3E). To explore mechanisms underlying GZMK⁺

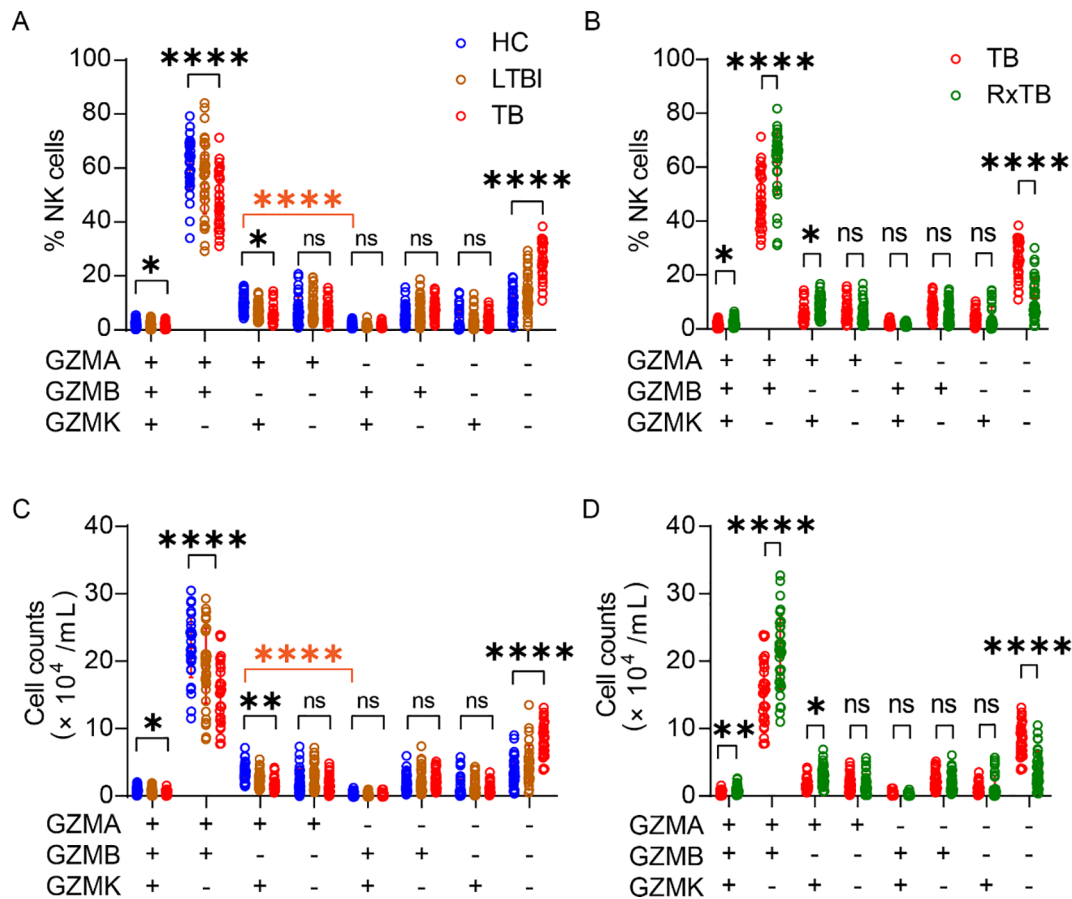


FIGURE 2

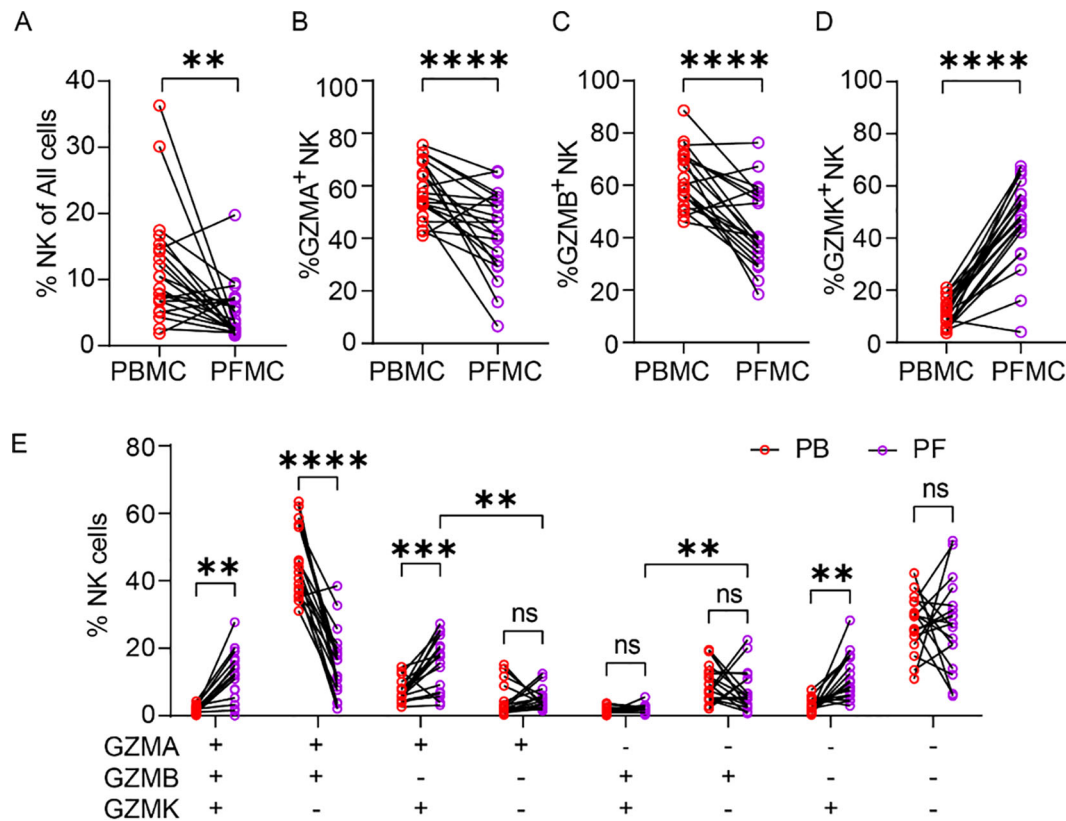
Co-expression of granzymes in peripheral blood NK cells during TB progression. (A, B) Frequency of triple-granzyme co-expressing NK cells was evaluated using Boolean gating in FlowJo. (C, D) Absolute count of triple-granzyme co-expressing NK cells, calculated from the total NK cell count and the percentage of granzyme-positive cells. Each dot represents an individual donor. Data are shown as mean \pm SEM, ns, not significant, * $P < 0.05$, ** $P < 0.01$, and **** $P < 0.0001$ by one-way ANOVA with Tukey's multiple comparisons test (A, C) or unpaired Student's t-test (B, D). The orange asterisks in (A, C) denote significant differences between GZMA⁺GZMB⁻GZMK⁺ and GZMA⁻GZMB⁺GZMK⁺ NK cell populations in healthy controls, as assessed by unpaired Student's t-test.

NK enrichment, we stimulated healthy donor PBMCs with *Mtb* strains (H37Ra or H37Rv), TGF- β (an NK activator abundant in TPE), or TB pleural fluid supernatant (PFS), either alone or combined with H37Rv. None of these stimuli significantly altered the frequency of GZMK⁺ NK cells (Supplementary Figures 3C–E). These results indicate that the distinct granzyme expression profiles in NK cells from the peripheral blood and pleural cavity of TB patients are not solely attributable to direct stimulation by *Mtb*, but likely reflect broader compartment-specific regulatory mechanisms.

Increased GZMK⁺ NK cells in pleural fluid arise from CD56^{bright} NK cell enrichment

Human NK cells are classified into CD56^{bright} and CD56^{dim} subsets, with CD56^{bright} NK cells lacking CD16 (FcyRIIIa), exhibiting low cytotoxicity, and secreting high levels of cytokines, whereas CD56^{dim} NK cells express CD16, demonstrate potent cytotoxicity, and produce fewer cytokines (27, 28). Given this established dichotomy, we further analyzed their granzyme expression in PBMC and PFMC compartments, as detailed in the gating strategy (Supplementary Figure 4). We observed distinct distribution patterns of GZMA, GZMB, and GZMK between

CD56^{bright} and CD56^{dim} subsets (Figures 4A–C). In PBMCs, GZMA and GZMB were predominantly expressed in CD56^{dim} NK cells and were significantly downregulated during active TB. In contrast, expression of these granzymes was minimal in CD56^{bright} NK cells and remained unaffected by TB status (Figures 4D, E). Conversely, GZMK expression was primarily restricted to CD56^{bright} NK cells and decreased significantly during TB, while remaining low and stable in CD56^{dim} subset (Figure 4F). Following treatment, the frequencies of GZMA⁺ CD56^{dim} and GZMK⁺ CD56^{bright} cells significantly rebounded, and GZMB⁺ CD56^{dim} cells also showed a trending increase (Figures 4G–I). In PFMCs, the proportions of GZMA⁺ cells were uniformly low across CD56^{dim} and CD56^{bright} subsets without inter-subset differences (Figure 4J). GZMB expression remained preferentially associated with CD56^{dim} NK cells, similar to the pattern in PBMCs (Figure 4K), while GZMK expression remained highest in CD56^{bright} subsets (Figure 4L), mirroring PBMC distribution. Importantly, PFMCs contained a significantly lower proportion of CD56^{dim} NK cells and a correspondingly higher frequency of CD56^{bright} NK cell compared to matched PBMCs (Figures 4M, N), consistent with prior reports (29). Collectively, these findings suggest that the higher frequency of GZMK⁺ NK cells



in PFMCs compared with PBMCs is attributable to the enrichment of CD56^{bright} NK cells, which are the primary GZMK-expressing subset.

Granzyme expression patterns differ between CD56^{bright} and CD56^{dim} NK subsets and exhibit distinct changes during TB progression

To delineate subset-specific profiles, we separately analyzed the co-expression patterns of GZMA, GZMB, and GZMK within CD56^{dim} and CD56^{bright} NK cells. Within the CD56^{dim} subset, the GZMA⁺GZMB⁺GZMK⁻ phenotype was the predominant population, accounting for a significantly higher proportion than all other subsets (Figure 5A). Notably, among CD56^{dim} compartment, both the frequencies and absolute numbers of GZMA⁺GZMB⁺GZMK⁺ and GZMA⁺GZMB⁺GZMK⁻ NK cells decreased during active TB and recovered post-treatment (Figures 5A, B, Supplementary Figures 5A, B). In contrast to the pattern observed in total NK cells, the GZMA⁺GZMB⁻GZMK⁺ population within CD56^{dim} cells did not change significantly during disease progression and remained low in frequency (Figures 2A, 5A). Mirroring the trend in total NK cells, the percentage and absolute number of GZMA⁻GZMB⁻GZMK⁻ CD56^{dim} NK cells increased during active TB and decreased after therapy

(Figures 2, 5A, B, Supplementary Figures 5A, B). Additionally, although the frequency of the GZMA⁻GZMB⁺GZMK⁻ subset was unaltered by disease state, its absolute count was reduced in TB patients (Supplementary Figure 5A).

In contrast to CD56^{dim} NK cells, CD56^{bright} NK cells displayed a distinct granzyme co-expression profile and disease-associated pattern. The dominant subsets within CD56^{bright} NK cells were GZMA⁺GZMB⁻GZMK⁺ and GZMA⁻GZMB⁻GZMK⁺, both of which showed marked reductions during TB progression and significant recovery after treatment (Figures 5C, D). The GZMA⁺GZMB⁺GZMK⁻ subset was present at low frequencies in CD56^{bright} NK cells and did not exhibit the TB-associated changes observed in total NK cells (Figures 2A, 5C). Although the frequency of GZMA⁻GZMB⁻GZMK⁻ CD56^{bright} NK cells increased during active TB and declined after treatment, their absolute numbers did not change significantly across disease stages (Figures 5C, D, Supplementary Figures 5C, D). Importantly, the absolute counts of several CD56^{bright} NK cell subsets, including GZMA⁺GZMB⁺GZMK⁺, GZMA⁺GZMB⁺GZMK⁻, GZMA⁺GZMB⁻GZMK⁺, GZMA⁻GZMB⁺GZMK⁻, and GZMA⁻GZMB⁻GZMK⁺ were decreased during active TB (Supplementary Figure 5C), providing further evidence that CD56^{bright} NK cells are reduced in peripheral blood over the course of disease progression.

Comparative analysis of granzyme expression in CD56^{dim} and CD56^{bright} subsets between PBMCs and PFMCs revealed further

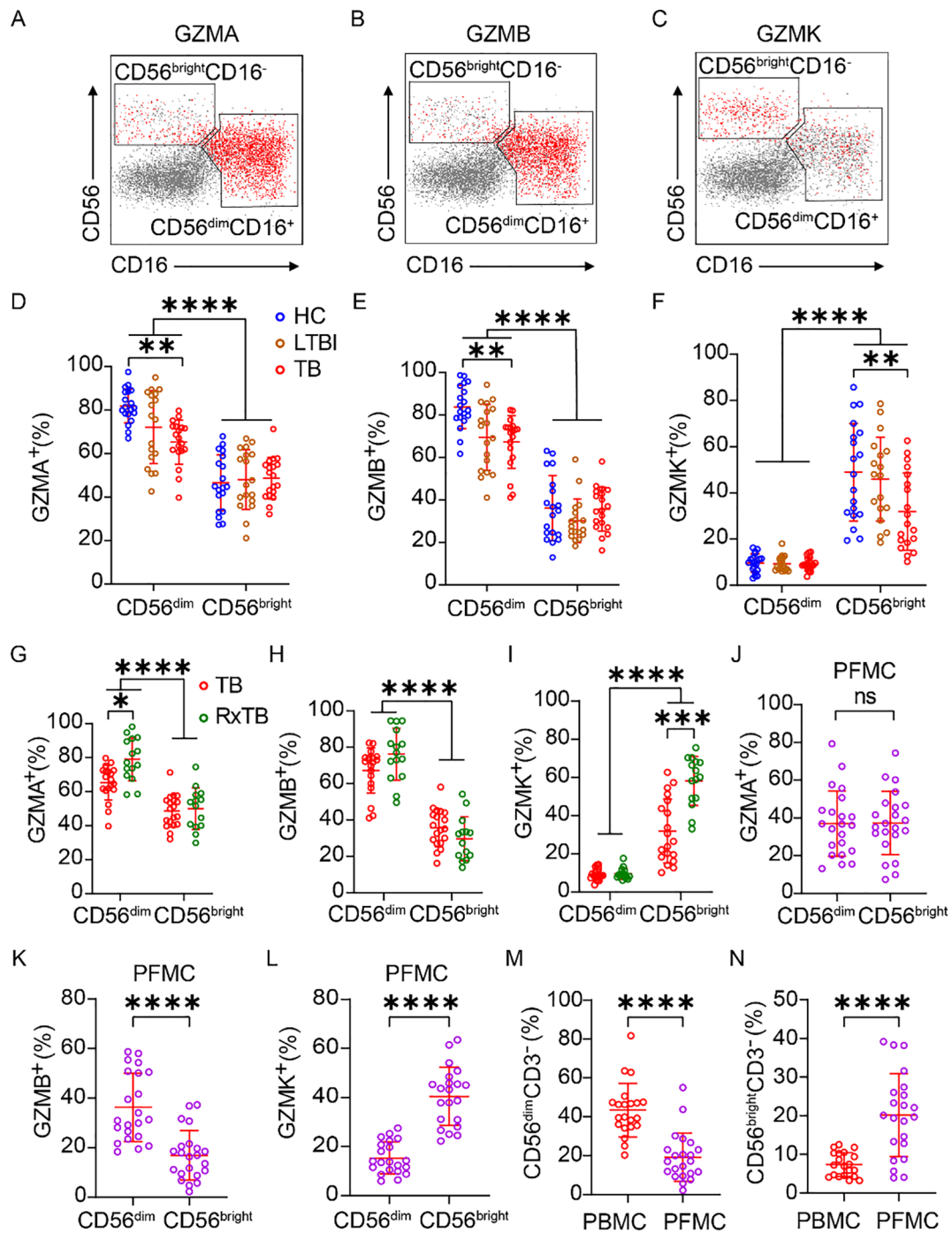


FIGURE 4

Increased GZMK⁺ NK cells in pleural fluid Arise from CD56^{bright} NK cell enrichment. (A–G) Representative biaxial flow cytometry plots of CD56 versus CD16 showing granzyme⁺ (red) and granzyme[−] (gray) NK cells. Panels illustrate GZMA (A), GZMB (B) and GZMK (C) distributions. (D–I) Frequency of GZMA⁺, GZMB⁺, and GZMK⁺ cells within the CD56^{bright} and CD56^{dim} NK subsets in PBMCs samples from HC, LTBI, TB and RxTB patient. (J–L) Frequency of GZMA⁺, GZMB⁺, and GZMK⁺ cells within the CD56^{bright} and CD56^{dim} subsets in PFMCs samples from TPE patient. (M, N) Comparison of overall CD56^{bright} and CD56^{dim} NK cell frequencies between matched PBMCs and PFMCs. Each dot represents one donor. Data are shown as means ± SEM, ns, not significant, **P* < 0.05, ***P* < 0.01, ****P* < 0.001, and *****P* < 0.0001. Comparisons between CD56^{bright} and CD56^{dim} subsets within the same clinical group were analyzed by two-way ANOVA with Tukey’s multiple comparisons test (D–I). Comparisons across clinical groups within the CD56^{bright} or CD56^{dim} subsets were analyzed by one-way ANOVA with Tukey’s multiple comparisons test (D–I). Unpaired Student’s *t*-test was used for paired-compartment analyses (J–N).

distinctions. In CD56^{dim} NK cells, the GZMA⁺GZMB⁺GZMK⁺ and GZMA⁺GZMB[−]GZMK⁺ subsets were significantly enriched in PFMCs, whereas the predominant GZMA⁺GZMB⁺GZMK[−] subset was markedly reduced, consistent with the distribution observed in

total NK cells (Figures 3E, 5E). In contrast, CD56^{bright} NK cells showed no significant differences in the frequencies of GZMA⁺GZMB⁺GZMK⁺ or GZMA⁺GZMB[−]GZMK⁺ subsets between PBMCs and PFMCs. However, the GZMA[−]GZMB[−]

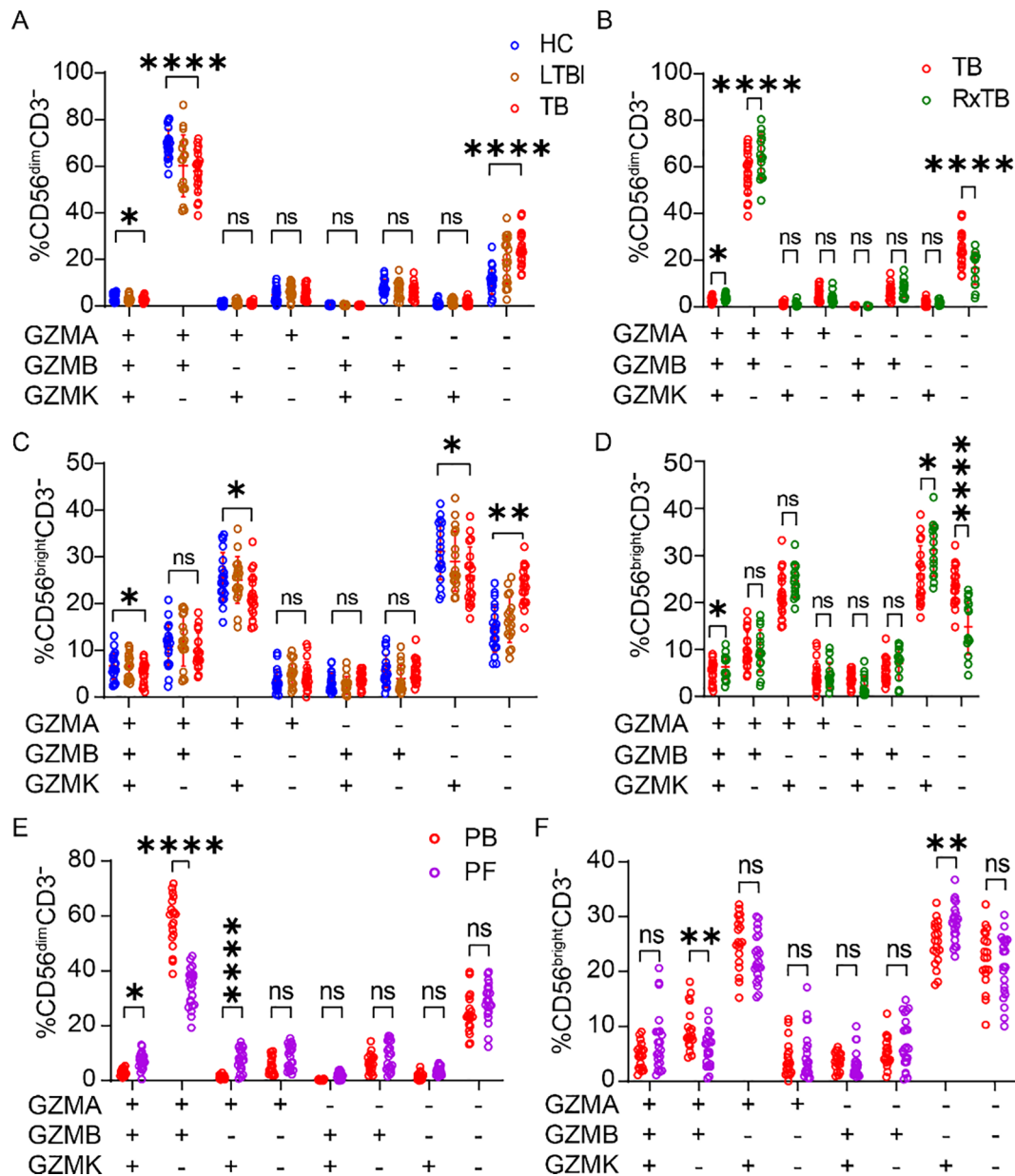


FIGURE 5 Granzyme co-expression within CD56^{dim} and CD56^{bright} NK cell subsets. (A, B) Frequency of triple-granzyme co-expressing cells within the CD56^{dim} NK cell subset from PBMCs of different donor groups (HC, LTBI, TB in A; TB and RxTB in B). (C, D) Frequency of triple-granzyme co-expressing cells within the CD56^{bright} NK cell subset from PBMCs of different donor groups (HC, LTBI, TB in C; TB and RxTB in D). (E, F) Comparison of triple-granzyme co-expressing cells between PBMCs and PFMCs in TB patients, within CD56^{dim} (E) and CD56^{bright} (F) subsets. Each dot represents an individual donor. Data are shown as mean ± SEM, ns, not significant, **P* < 0.05, ***P* < 0.01, and *****P* < 0.0001 by one-way ANOVA with Tukey's multiple comparisons test (A, C) or unpaired Student's *t*-test (B, D–F).

GZMK⁺ subset was significantly enriched in PFMCs (Figure 5F), further supporting the notion that the increased abundance of GZMK⁺ NK cells in pleural fluid is primarily driven by the enrichment of CD56^{bright} NK cells at the site of infection.

CCR5^{bright}-associated redistribution of GZMK⁺CD56^{bright} NK cells from circulation to the pleural space in active tuberculosis

To investigate the mechanistic basis for increased CD56^{bright} NK cell frequencies in PFMCs relative to PBMCs, we first examined peripheral

CD56 subset dynamics across clinical stages. The proportions and absolute count of CD56^{bright} NK cell in peripheral blood were reduced in active TB but returned to baseline after treatment (Figure 6A, Supplementary Figure 6A), whereas CD56^{dim} frequencies and absolute counts showed no significant change (Supplementary Figures 6B, C). We therefore hypothesized that CD56^{bright} NK cells in peripheral blood migrate into the pleural compartment during disease progression. Previous studies have identified a CCR5^{bright} CD4⁺ effector memory cells that exhibits exceptionally high GZMK expression (30). CCR5 interacts with multiple CC chemokines, including CCL2, CCL3, CCL7 and CCL8 (31), which are significantly enriched in the pleural

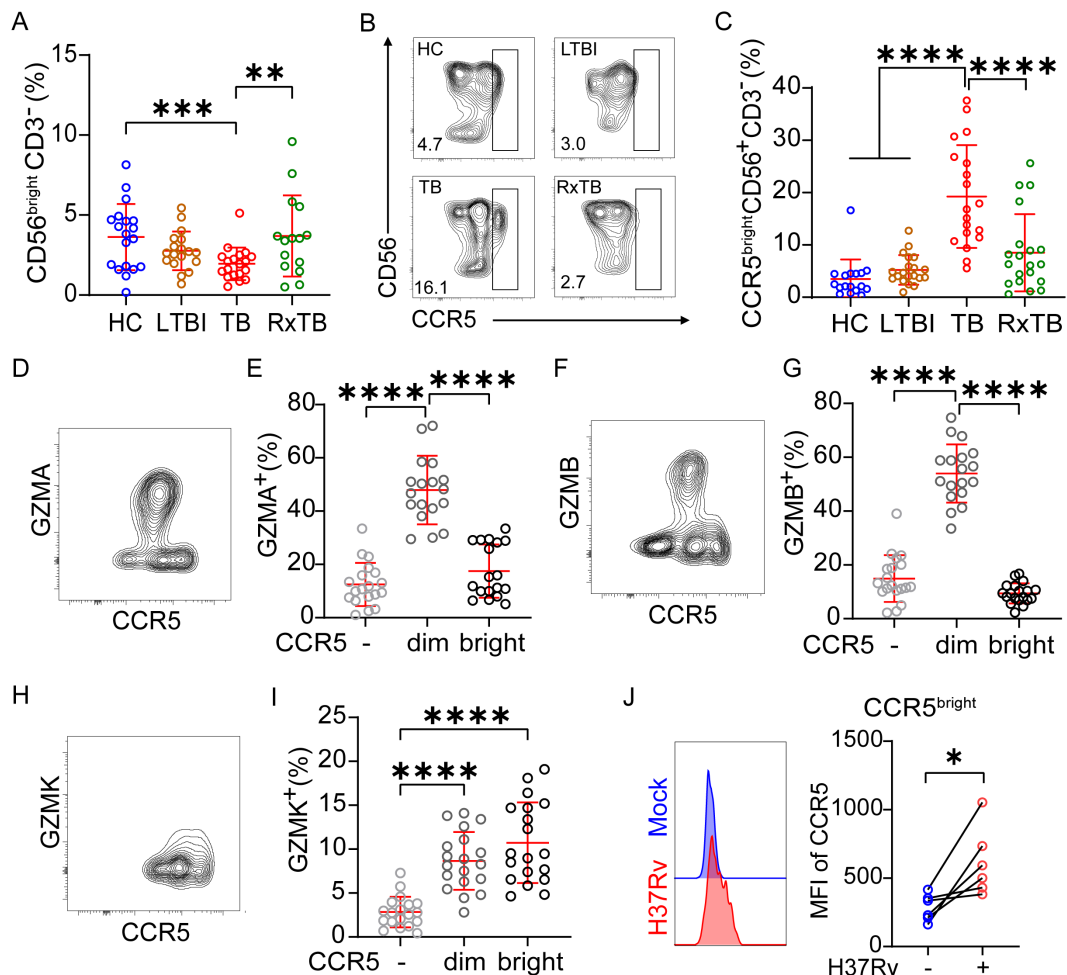


FIGURE 6

CCR5^{bright} NK cells are preferentially GZMK⁺ and increase during active TB. (A) Frequencies of CD56^{bright} NK cell subsets in PBMCs from HCs, LTBI, TB, and RxTB. (B) Contour plots showing CD56 versus CCR5 expression on CD3⁻ cells from different donor groups. CD56⁺CCR5⁺ cells in TB patients can be classified into three distinct subsets: CCR5⁻, CCR5^{dim}, and CCR5^{bright}. (C) Percentages of CCR5^{bright} cells among CD56⁺CD3⁻ cells. The CCR5^{bright} subset was significantly increased in active TB patients compared to HCs, LTBI individuals, and RxTB patients. (D, F, H) Contour plots illustrating granzyme expression versus CCR5 in NK cells from TB patients. (E, G, I) Proportions of GZMA⁺, GZMB⁺ and GZMK⁺ NK cells within CCR5-defined subsets. GZMK⁺ NK cells were preferentially enriched in the CCR5^{bright} population, whereas GZMA⁺ and GZMB⁺ distributions showed no such bias. (J) Following *ex vivo* H37Rv infection (MOI = 5, 24 h), mean fluorescence intensity (MFI) of CCR5 increased significantly on CD56^{bright} NK cells. Data are shown as means \pm SEM, ns, not significant, * P < 0.05, ** P < 0.01, *** P < 0.001, and **** P < 0.0001 by one-way ANOVA with Tukey's multiple comparisons test (A, C, E, G, I) or unpaired Student's *t*-test (J).

fluid of TB patients (32–34). On this basis, we asked whether CCR5 mediate GZMK⁺NK-cell subset migration.

Contour plots of CD56 versus CCR5 revealed two distinct subsets among CD56⁺ cells in HC, LTBI, and RxTB groups, whereas TB patients exhibited three subsets based on CCR5 expression levels (Figure 6B, Supplementary Figure 6D), which we designated as CCR5⁻, CCR5^{dim}, and CCR5^{bright}, paralleling previous observations in CCR5^{bright} CD4⁺ effector memory T cells (30). Using the gating strategy outlined in Supplementary Figure 6D, we analyzed the frequency and absolute count of CCR5^{bright} cells within CD3⁻CD56⁺ NK cells. Relative to HCs and LTBI subjects, the CCR5^{bright} NK subset exhibited a significant increase in both percentage and absolute number in active TB patients, which substantially declined after treatment (Figure 6C, Supplementary Figure 6E), suggesting that this increase was not attributable to a contraction of other NK subpopulations. We

further evaluated granzyme expression profiles across these CCR5-defined NK subpopulations in TB patients. GZMA and GZMB were predominantly expressed in CCR5^{dim} NK cells and were significantly lower in both CCR5⁻ and CCR5^{bright} subsets (Figures 6D–G). In contrast, GZMK was highly expressed in both CCR5^{dim} and CCR5^{bright} NK cells (Figures 6H, I). Additionally, *In vitro* H37Rv stimulation significantly augmented CCR5 surface density (mean fluorescence intensity, MFI) specifically on CD56^{bright} NK cells derived from healthy donor PBMCs (Figure 6J), with no significant effect observed on the CD56^{dim} subset (Supplementary Figure 6F). Together, these data indicate that TB progression selectively expands a CCR5^{bright} NK subset with high GZMK but low GZMA/GZMB. This specific phenotype aligns with pleural fluid enrichment profiles, supporting a CCR5-dependent trafficking model for GZMK⁺CD56^{bright} NK cells from circulation to the pleural space.

Discussion

Clinical and single-cell studies consistently report altered NK cell frequency and function during TB progression, with partial recovery following treatment (12, 21, 35). Our data extend these observations by demonstrating a coordinated downregulation in both the frequency and absolute numbers of NK cells co-expressing GZMA, GZMB and GZMK in PBMC-derived NK cells from active TB patients, with partial or full recovery after therapy. Moreover, we reveal a compartment-specific remodeling of granzyme expression: pleural fluid NK cells exhibited significantly elevated GZMK but diminished GZMA and GZMB compared to their blood counterparts. The enrichment of GZMK⁺CD56^{bright} NK cells in pleural effusions was further associated with the expansion of a distinct CCR5^{bright} NK population in TB patients.

Natural killer (NK) cells are rapid, non-MHC-restricted effectors of innate immunity and play a critical role in early host defense against *Mtb* (22). Previous studies have reported a decline in NK cell numbers during the transition from latent infection to active disease, with recovery following treatment (15). Single-cell sequencing has further identified selective depletion of peripheral CD7⁺GZMB⁺CD3⁻ cells (mainly NK cells) in active TB, distinguishing active TB from LTBI and healthy controls (25). Additionally, circulating NK cells from TB patients exhibit impaired IFN- γ production, which improves after therapy (18, 20, 36). Our data extend these findings by revealing that NK cell dysfunction in active TB is characterized not only by numerical changes but also by a profound functional impairment, evidenced by a broad reduction in granzyme-co-expressing subsets at both the frequency and absolute count levels.

Importantly, our subset analysis reveals that granzyme expression patterns differ fundamentally between CD56^{dim} and CD56^{bright} NK subsets and exhibit distinct changes during TB progression. The loss of cytotoxic potential during active disease was primarily driven by changes within the CD56^{dim} subset, including the reduction of major co-expressing populations like GZMA⁺GZMB⁺GZMK⁻. In contrast, the CD56^{bright} subset, which naturally expresses high GZMK but low GZMA/GZMB, showed a different pattern of change. This subset-specific granularity clarifies the overall granzyme landscape and underscores that TB-associated NK cell dysfunction is not uniform across all subsets.

NK cells reside in various tissues, where they contribute to organ-specific immune responses (37–39). In the case of TB, the lungs serve as the primary site of infection and a gateway for extrapulmonary dissemination (40). However, research on PFMC-derived NK cells in TB remain scarce. Consistent with previous work (29), Our paired analysis found that PFMCs contain fewer NK cells overall, a higher proportion of CD56^{bright} CD16⁻ NK cells, and a lower proportion of CD56^{dim} CD16⁺ NK cells than matched PBMCs. Consequently, GZMK⁺ NK cells are enriched in PFMCs, reflecting the predominance of the CD56^{bright} subset, while GZMA⁺ and GZMB⁺ NK cells are diminished, aligning with their association with the CD56^{dim} subset. Chemokine-driven recruitment plays a critical role in the effective immune response against *Mtb*. In mice infected with *Mtb*, CCR5-expressing cells, including lymphocytes and macrophages, infiltrate the lungs (41). CCR5 interacts with

multiple ligands, such as CCL2, CCL3, CCL5, CCL7, and CCL8 (31). In TB patients, monocytes derived from lymph node tissues and alveolar macrophages produce higher levels of CCL2, CCL3, and CCL5 than those from peripheral blood (42). Similarly, tuberculous pleural effusions contain significantly elevated levels of CCL2, CCL3, and CCL7 compared to effusions caused by other diseases (32, 33). CCL8 is also markedly higher in TB pleural fluid than in peripheral blood (34). Thus, we speculate that CCR5 may mediate the recruitment of CD56^{bright} NK cells into the pleural space in response to these chemokines. Our study identifies an increased frequency of a CCR5^{bright} NK cells in peripheral blood from active TB patients. The CCR5^{bright} subset is enriched for GZMK but not GZMA or GZMB, echoing observations in CCR5^{bright} CD4⁺ effector memory T cells (30). *In vitro* infection with H37Rv selectively increased CCR5 expression on CD56^{bright} NK cells without affecting the CD56^{dim} subset. This suggests that CCR5^{bright} NK cells, enriched for GZMK, may migrate from the circulation into pleural space, where their peripheral fraction is reduced in active TB.

In summary, while previous studies have documented NK-cell depletion in TB, our research highlights a complementary functional deficit in NK cells, specifically a reduction in granzyme-expressing subsets. We provide the first comprehensive characterization of granzyme profiles in pleural NK cells, linking their distinct pattern to the differential distribution of CD56 subsets. Furthermore, we identify an expansion of CCR5^{bright} NK cells in active TB, enriched for GZMK and associated with compartmental migration. These findings suggest that granzyme remodeling and CCR5-mediated trafficking are key mechanisms reshaping NK cell function and distribution in TB.

Methods

Ethics statement

This study received approval from the Ethics Committee of Shenzhen Third People's Hospital, and Board of the Shenzhen University School of Medicine, China. All participants provided written informed consent. Experimental procedures strictly adhered to institutional ethical guidelines and biosafety protocols.

Participants

Peripheral blood samples were collected from HC (n = 34), LTBI (n = 34), and patients with active TB (n = 30) admitted to Shenzhen Third People's Hospital (China) between August 2021 and March 2024. None of the active TB patients had a prior history of TB or anti-TB treatment at the time of enrollment. An additional cohort of patients who had received 1 to 10 months of RxTB (n = 34) was also recruited. Active TB was diagnosed based on clinical symptoms, chest radiography, positive sputum smear or culture for *Mtb*, and clinical response to anti-TB therapy. A validated IFN- γ ELISPOT assay specific for *Mtb* (IGRA) was used to distinguish LTBI cases from uninfected HCs (25). Additionally, paired PBMCs and PFMCs were obtained from 21 patients with TPE for flow

cytometric analysis and NK cell isolation. TPE was confirmed by the presence of exudative pleural fluid with culture-positive results for *Mtb* (from pleural fluid, pleural biopsy, or sputum), and/or by histological evidence of granulomatous inflammation with acid-fast bacilli on pleural biopsy.

Isolation and processing of PBMCs and PFCMs

Heparinized peripheral blood was collected via venipuncture from all participants. pleural fluid was obtained from patients diagnosed with TPE. PBMCs were isolated by density gradient centrifugation using Ficoll-Paque Plus (Amersham Biosciences). PFCMs and PFS were collected by centrifuging up to 50 mL of pleural fluid at $300 \times g$ for 5 minutes at 4 °C. Freshly isolated PBMCs and PFCMs were either immediately processed for flow cytometry or used for NK cell isolation via magnetic separation. PFS were stored at -80 °C for subsequent analyses. For *in vitro* stimulation assays, PBMCs from HCs were incubated for 24 hours with H37Rv, H37Ra, TGF- β , 20% PFS, alone or in combination (H37Rv + TGF- β , H37Rv + 20% PFS), according to the experimental design. After stimulation, cells were harvested for flow cytometric analysis as described below.

Flow cytometry and intracellular cytokine staining

PBMCs and PFCMs from TB patients were stained for surface and intracellular markers using standard protocols (24). Surface staining was performed using monoclonal antibodies against CD3 (clone SK-7, BioLegend #344816), CD16 (3G8, BioLegend #302008), and CD56 (5.1H11, BioLegend #9362546), along with Ghost Dye (BioLegend #423102) for viability exclusion. Cells were incubated with antibodies for 30 minutes at 4 °C. After fixation and permeabilization (50 minutes at 4 °C), intracellular staining was performed using antibodies against granzyme A (GZMA; CB9, BioLegend #507215), granzyme B (GZMB; QA18A28, BioLegend #396414), and granzyme K (GZMK; GM26E7, BioLegend #370510). CCR5 was detected with HM-CCR5 (BioLegend, catalog #107018). All antibodies were validated by the manufacturer for flow cytometric applications. Stained cells were resuspended in 200 μ L of 2% paraformaldehyde, acquired using a BD FACSAria™ III flow cytometer with FACSDiva software (BD Biosciences), and analyzed with FlowJo v10. Granzyme co-expression was assessed using Boolean gating in FlowJo v10.

Statistical analysis

Sample size calculations and statistical analyses were performed using GraphPad Prism 8. Depending on their distribution, differences between two groups were analyzed using either the independent sample t-test or the Mann-Whitney U test. For multiple group comparisons, the ANOVA or Kruskal-Wallis test was applied, contingent on data normality. All hypothesis tests were two-sided, and a *p*-value of less than 0.05 was considered statistically significant.

Data availability statement

The original contributions presented in the study are included in the article/Supplementary Material. Further inquiries can be directed to the corresponding authors.

Ethics statement

The studies involving humans were approved by the Ethics Committee of Shenzhen Third People's Hospital, and Board of the Shenzhen University School of Medicine. The studies were conducted in accordance with the local legislation and institutional requirements. The participants provided their written informed consent to participate in this study.

Author contributions

FL: Software, Investigation, Conceptualization, Project administration, Writing – original draft, Formal Analysis, Data curation, Validation, Visualization, Methodology. YD: Resources, Visualization, Writing – original draft, Project administration, Funding acquisition, Validation. SX: Validation, Formal Analysis, Resources, Writing – original draft. RH: Formal Analysis, Writing – original draft, Methodology, Funding acquisition. XG: Investigation, Formal Analysis, Writing – review & editing. XH: Validation, Writing – original draft, Software, Methodology. SZ: Methodology, Conceptualization, Software, Writing – original draft. YC: Writing – review & editing, Project administration, Conceptualization, Funding acquisition, Supervision, Resources. XC: Writing – review & editing, Resources, Project administration, Funding acquisition, Supervision. JH: Writing – review & editing, Funding acquisition, Project administration.

Funding

The author(s) declared that financial support was received for this work and/or its publication. This work was supported by grants from the Shenzhen Medical Research Funding Program (Nos. B2302035, A2302004 to XC and YC), the National Natural Science Foundation of China (Nos. 82430074, 82472294 to XC and YC), the Science and Technology Innovation Commission of Shenzhen (Nos. JCYJ20220818095610021, JSGG20220822095200001 to YC), the National Science Foundation of Jiangxi Province (No. 20212BAB206077 to RH), the Science and Technology Project of Guangdong Province (No. 2025A1515010675 to YD), the Science and Technology Research Project of the Education Department of Jiangxi Province (No. GJJ2501322 to FL), and the Ganzhou Key Research and Development Project (No. GZ2024YLJ118 to JH). The funders had no role in the study design, data collection and analysis, decision to publish, or preparation of the manuscript.

Conflict of interest

The author(s) declared that this work was conducted in the absence of any commercial or financial relationships that could be construed as a potential conflict of interest.

Generative AI statement

The author(s) declared that generative AI was not used in the creation of this manuscript.

Any alternative text (alt text) provided alongside figures in this article has been generated by Frontiers with the support of artificial intelligence and reasonable efforts have been made to ensure accuracy, including review by the authors wherever possible. If you identify any issues, please contact us.

References

- World Health, O. *Global tuberculosis report 2024*. Geneva: World Health Organization (2024).
- Litvinenko S, Magwood O, Wu S, Wei X. Burden of tuberculosis among vulnerable populations worldwide: an overview of systematic reviews. *Lancet Infect Dis.* (2023) 23:1395–407. doi: 10.1016/S1473-3099(23)00372-9
- Dotiwala F, Sen Santara S, Binker-Cosen AA, Li B, Chandrasekaran S, Lieberman J. Granzyme B disrupts central metabolism and protein synthesis in bacteria to promote an immune cell death program. *Cell.* (2017) 171:1125–37.e11. doi: 10.1016/j.cell.2017.10.004
- Lu C-C, Wu T-S, Hsu Y-J, Chang C-J, Lin C-S, Chia J-H, et al. NK cells kill mycobacteria directly by releasing perforin and granzysin. *J Leukoc Biol.* (2014) 96:1119–29. doi: 10.1189/jlb.4A0713-363RR
- Cooper MA, Fehniger TA, Caligiuri MA. The biology of human natural killer-cell subsets. *Trends Immunol.* (2001) 22:633–40. doi: 10.1016/S1471-4906(01)02060-9
- Gerosa F, Baldani-Guerra B, Nisii C, Marchesini V, Carra G, Trinchieri G. Reciprocal activating interaction between natural killer cells and dendritic cells. *J Exp Med.* (2002) 195:327–33. doi: 10.1084/jem.20010938
- Vankayalapati R, Klucar P, Wizel B, Weis SE, Samten B, Safi H, et al. NK cells regulate CD8+ T cell effector function in response to an intracellular pathogen. *J Immunol.* (2004) 172:130–7. doi: 10.4049/jimmunol.172.1.130
- Zhang R, Zheng X, Li B, Wei H, Tian Z. Human NK cells positively regulate gammadelta T cells in response to Mycobacterium tuberculosis. *J Immunol.* (2006) 176:2610–6. doi: 10.4049/jimmunol.176.4.2610
- Roy S, Barnes PF, Garg A, Wu S, Cosman D, Vankayalapati R. NK cells lyse T regulatory cells that expand in response to an intracellular pathogen. *J Immunol.* (2008) 180:1729–36. doi: 10.4049/jimmunol.180.3.1729
- Jaron B, Maranghi E, Leclerc C, Majlessi L. Effect of attenuation of Treg during BCG immunization on anti-mycobacterial Th1 responses and protection against Mycobacterium tuberculosis. *PLoS One.* (2008) 3:e2833. doi: 10.1371/journal.pone.0002833
- Feng CG, Kaviratne M, Rothfuchs AG, Cheever A, Hieny S, Young HA, et al. NK cell-derived IFN-gamma differentially regulates innate resistance and neutrophil response in T cell-deficient hosts infected with Mycobacterium tuberculosis. *J Immunol.* (2006) 177:7086–93. doi: 10.4049/jimmunol.177.10.7086
- Wang Y, Sun Q, Zhang Y, Li X, Liang Q, Guo R, et al. Systemic immune dysregulation in severe tuberculosis patients revealed by a single-cell transcriptome atlas. *J Infect.* (2023) 86:421–38. doi: 10.1016/j.jinf.2023.03.020
- Leung WL, Law KL, Leung VSS, Yip CW, Leung CC, Tam CM, et al. Comparison of intracellular cytokine flow cytometry and an enzyme immunoassay for evaluation of cellular immune response to active tuberculosis. *Clin Vaccine Immunol.* (2009) 16:344–51. doi: 10.1128/CVI.00159-08
- Morais-Papini TF, Coelho-Dos-Reis JGA, Wendling APB, do Vale Antonelli LR, Wovk PF, Bonato VLD, et al. Systemic Immunological changes in patients with distinct clinical outcomes during Mycobacterium tuberculosis infection. *Immunobiology.* (2017) 222:1014–24. doi: 10.1016/j.imbio.2017.05.016
- Roy Chowdhury R, Vallania F, Yang Q, Lopez Angel CJ, Darboe F, Penn-Nicholson A, et al. A multi-cohort study of the immune factors associated with M.

Publisher's note

All claims expressed in this article are solely those of the authors and do not necessarily represent those of their affiliated organizations, or those of the publisher, the editors and the reviewers. Any product that may be evaluated in this article, or claim that may be made by its manufacturer, is not guaranteed or endorsed by the publisher.

Supplementary material

The Supplementary Material for this article can be found online at: <https://www.frontiersin.org/articles/10.3389/fimmu.2026.1747972/full#supplementary-material>

- tuberculosis infection outcomes. *Nature.* (2018) 560:644–8. doi: 10.1038/s41586-018-0439-x
- Bozzano F, Costa P, Passalacqua G, Dodi F, Ravera S, Pagano G, et al. Functionally relevant decreases in activatory receptor expression on NK cells are associated with pulmonary tuberculosis in vivo and persist after successful treatment. *Int Immunol.* (2009) 21:779–91. doi: 10.1093/intimm/dxp046
- Mehanna N, Pradhan A, Kaur R, Kontopoulos T, Rosati B, Carlson D, et al. CD8 α marks a Mycobacterium tuberculosis-reactive human NK cell population with high activation potential. *Sci Rep.* (2025) 15:15095. doi: 10.1038/s41598-025-98367-4
- Wang F, Hou H, Wu S, Tang Q, Huang M, Yin B, et al. Tim-3 pathway affects NK cell impairment in patients with active tuberculosis. *Cytokine.* (2015) 76:270–9. doi: 10.1016/j.cyto.2015.05.012
- Albayrak N, Dirix V, Aerts L, Van Praet A, Godefroid A, Dauby N, et al. Differential expression of maturation and activation markers on NK cells in patients with active and latent tuberculosis. *J Leukoc Biol.* (2022) 111:1031–42. doi: 10.1002/JLB.4A1020-641RR
- Nirmala R, Narayanan PR, Mathew R, Maran M, Devan CN. Reduced NK activity in pulmonary tuberculosis patients with/without HIV infection: identifying the defective stage and studying the effect of interleukins on NK activity. *Tuberculosis.* (2001) 81:343–52. doi: 10.1054/tube.2001.0309
- Schierloh P, Alemán M, Yokobori N, Alves L, Roldán N, Abbate E, et al. NK cell activity in tuberculosis is associated with impaired CD11a and ICAM-1 expression: a regulatory role of monocytes in NK activation. *Immunology.* (2005) 116:541–52. doi: 10.1111/j.1365-2567.2005.02259.x
- Chen S, Zhu H, Jounaidi Y. Comprehensive snapshots of natural killer cells functions, signaling, molecular mechanisms and clinical utilization. *Signal Transduct Target Ther.* (2024) 9:302. doi: 10.1038/s41392-024-02005-w
- Rasi V, Phelps KR, Paulson KR, Eickhoff CS, Chinnaraj M, Pozzi N, et al. Homodimeric Granzyme A Oponizes Mycobacterium tuberculosis and Inhibits Its Intracellular Growth in Human Monocytes via Toll-Like Receptor 4 and CD14. *J Infect Dis.* (2024) 229:876–87. doi: 10.1093/infdis/jiad378
- Cai Y, Wang Y, Shi C, Dai Y, Li F, Xu Y, et al. Single-cell immune profiling reveals functional diversity of T cells in tuberculous pleural effusion. *J Exp Med.* (2022) 219(3): e20211777. doi: 10.1084/jem.20211777
- Cai Y, Dai Y, Wang Y, Yang Q, Guo J, Wei C, et al. Single-cell transcriptomics of blood reveals a natural killer cell subset depletion in tuberculosis. *EBioMedicine.* (2020) 53:102686. doi: 10.1016/j.ebiom.2020.102686
- Shaw JA, Diacon AH, Koegelenberg CFN. Tuberculous pleural effusion. *Respirology.* (2019) 24:962–71. doi: 10.1111/resp.13673
- Fauriat C, Long EO, Ljunggren H-G, Bryceson YT. Regulation of human NK-cell cytokine and chemokine production by target cell recognition. *Blood.* (2010) 115:2167–76. doi: 10.1182/blood-2009-08-238469
- Long EO, Kim HS, Liu D, Peterson ME, Rajagopalan S. Controlling natural killer cell responses: integration of signals for activation and inhibition. *Annu Rev Immunol.* (2013) 31:227–58. doi: 10.1146/annurev-immunol-020711-075005
- Schierloh P, Yokobori N, Alemán M, Musella RM, Beigier-Bompadre M, Saab MA, et al. Increased susceptibility to apoptosis of CD56dimCD16+ NK cells induces the

- enrichment of IFN-gamma-producing CD56bright cells in tuberculous pleurisy. *J Immunol.* (2005) 175:6852–60. doi: 10.4049/jimmunol.175.10.6852
30. Herich S, Schneider-Hohendorf T, Rohlmann A, Khaleghi Ghadiri M, Schulte-Mecklenbeck A, Zondler L, et al. Human CCR5high effector memory cells perform CNS parenchymal immune surveillance via GZMK-mediated transendothelial diapedesis. *Brain.* (2019) 142:3411–27. doi: 10.1093/brain/awz301
31. Liu S, Liu N, Wang H, Zhang X, Yao Y, Zhang S, et al. CCR5 promoter polymorphisms associated with pulmonary tuberculosis in a Chinese Han population. *Front Immunol.* (2020) 11:544548. doi: 10.3389/fimmu.2020.544548
32. Mohammed KA, Nasreen N, Ward MJ, Mubarak KK, Rodriguez-Panadero F, Antony VB. Mycobacterium-mediated chemokine expression in pleural mesothelial cells: role of C-C chemokines in tuberculous pleurisy. *J Infect Dis.* (1998) 178:1450–6. doi: 10.1086/314442
33. Luo L, Deng S, Tang W, Hu X, Yin F, Ge H, et al. Monocytes subtypes from pleural effusion reveal biomarker candidates for the diagnosis of tuberculosis and Malignancy. *J Clin Lab Anal.* (2022) 36:e24579. doi: 10.1002/jcla.24579
34. Liu H, Liu Z, Chen J, Chen L, He X, Zheng R, et al. Induction of CCL8/MCP-2 by mycobacteria through the activation of TLR2/PI3K/Akt signaling pathway. *PLoS One.* (2013) 8:e56815. doi: 10.1371/journal.pone.0056815
35. Wang J, Chai Q, Lei Z, Wang Y, He J, Ge P, et al. LILRB1-HLA-G axis defines a checkpoint driving natural killer cell exhaustion in tuberculosis. *EMBO Mol Med.* (2024) 16:1755–90. doi: 10.1038/s44321-024-00106-1
36. Garand M, Goodier M, Owolabi O, Donkor S, Kampmann B, Sutherland JS. Functional and Phenotypic Changes of Natural Killer Cells in Whole Blood during Mycobacterium tuberculosis Infection and Disease. *Front Immunol.* (2018) 9:257. doi: 10.3389/fimmu.2018.00257
37. Freud AG, Mundy-Bosse BL, Yu J, Caligiuri MA. The broad spectrum of human natural killer cell diversity. *Immunity.* (2017) 47:820–33. doi: 10.1016/j.immuni.2017.10.008
38. Peng H, Tian Z. Diversity of tissue-resident NK cells. *Semin Immunol.* (2017) 31:3–10. doi: 10.1016/j.smim.2017.07.006
39. Stamatziades EG, Li MO. Tissue-resident cytotoxic innate lymphoid cells in tumor immunosurveillance. *Semin Immunol.* (2019) 41:101269. doi: 10.1016/j.smim.2019.03.001
40. Elkington PT, Friedland JS. Permutations of time and place in tuberculosis. *Lancet Infect Dis.* (2015) 15:1357–60. doi: 10.1016/S1473-3099(15)00135-8
41. Algood HM, Chan J, Flynn JL. Chemokines and tuberculosis. *Cytokine Growth Factor Rev.* (2003) 14:467–77. doi: 10.1016/S1359-6101(03)00054-6
42. Sadek MI, Sada E, Toossi Z, Schwander SK, Rich EA. Chemokines induced by infection of mononuclear phagocytes with mycobacteria and present in lung alveoli during active pulmonary tuberculosis. *Am J Respir Cell Mol Biol.* (1998) 19:513–21. doi: 10.1165/ajrcmb.19.3.2815